Supplementary Information for:
Grazing Incidence Transmission X-ray Scattering: Surface Scattering in the Born Approximation

Xinhui Lu, Kevin G. Yager, Danvers E. Johnston, Charles T. Black, and Benjamin M. Ocko

Refraction correction

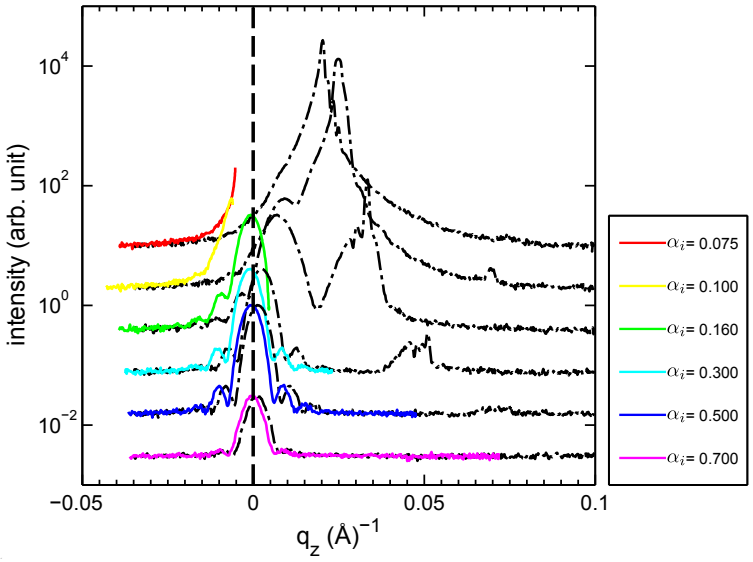

Figure 1: Refraction corrections of intensity profile of first order BRs for the fingerprint-patterned nanostructured sample at different incident angles. Black curves are before corrections and the colored ones are after corrections based on Eq. 1 (main text). This figure demonstrates that Eq. 1(main text) adequately corrects the refraction of the scattered beams with $\alpha_{ct} = 0.09°$ since the central peaks in the bottom four curves are now centered at $q_z = 0$.

Additional Corrections

Besides refraction correction, we describe a variety of corrections to the data (intensity and q-scale) which were considered and found to be negligible for typical experimental conditions for a Grazing-incidence Transmission Small-Angle X-ray Scattering (GTSAXS) experiment. These considerations could become relevant if a GTSAXS experiment is pushed to the edge of its applicability, in which case they would be crucial for quantitative data analysis.

Absorption Correction

First, we consider the asymmetry in absorption above and below the direct (refracted) beam, arising from the slightly different path-lengths of the scattered radiation through the absorbing substrate. The geometry is shown in the figure below.

The beam is incident onto the sample at angle α_i, and has a projected size along the sample surface of w. We define the x-axis to be along the beam propagation. A representative scattering

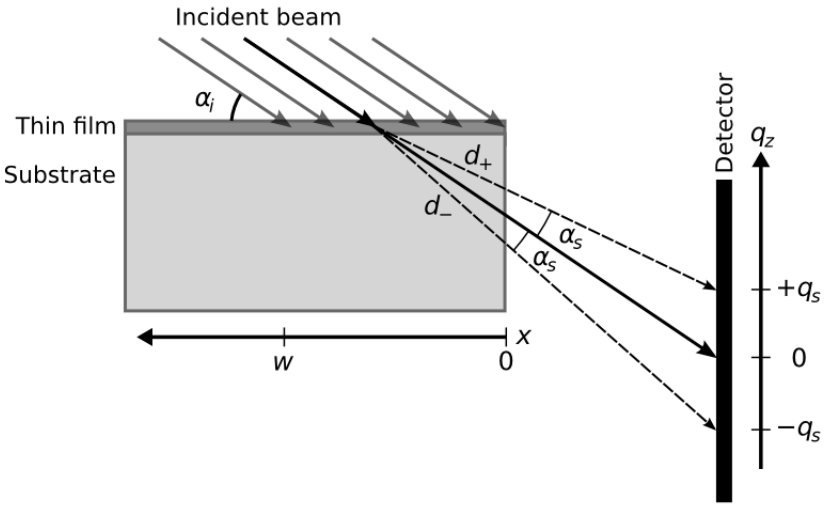

Figure 2: Geometry for GTSAXS. The pathlength through the substrate of the scattering below the direct beam is slightly longer than the scattering above the direct beam.

event is shown: the direct beam continues to the detector plane and defines $q_z = 0$. Scattering occurs both above and below the direct beam. For a scattering angle α_s (within the plane shown in Figure 2) this produces scattered intensity on the detector at $q_z = +q_s$ and $q_z = -q_s$. However the path of the scattered radiation through the substrate is not identical for these two reflections. In particular, the 'positive q_z' scattering travels a distance d_+ through the substrate, while the 'negative q_z' scattering travels a longer distance d_-:

$$d_+ = \frac{x}{\cos(\alpha_i - \alpha_s)} \tag{1}$$

$$d_- = \frac{x}{\cos(\alpha_i + \alpha_s)} \tag{2}$$

For a scattering intensity I_s, the measured scattering is attenuated by the substrate's absoprtion coefficient, ξ. The measured ratio of scattering intensities would be:

$$\frac{I_+}{I_-} = \frac{I_s e^{-\xi d_+}}{I_s e^{-\xi d_-}} \tag{3}$$

$$= \exp\left[-\xi \frac{x}{\cos(\alpha_i - \alpha_s)} + \xi \frac{x}{\cos(\alpha_i + \alpha_s)}\right] \tag{4}$$

$$= \exp\left[-\xi x \frac{\cos(\alpha_i + \alpha_s) - \cos(\alpha_i - \alpha_s)}{\cos(\alpha_i - \alpha_s)\cos(\alpha_i + \alpha_s)}\right] \tag{5}$$

$$= \exp\left[+\xi x \frac{\sin(\alpha_i)\sin(\alpha_s)}{\cos(\alpha_i - \alpha_s)\cos(\alpha_i + \alpha_s)}\right] \tag{6}$$

$$\tag{7}$$

An experimental scattering peak arises from the contributions of all rays in the incident beam. RAssuming a spatially uniform beam, all incident rays from the edge of the sample ($x = 0$) to the full beam projection ($x = w$) must be integrated with the appropriate absorption factor. This yields:

$$I_{+/-} = \frac{\int_{x=0}^{w} \frac{I_+}{I_-} \mathrm{d}x}{\int_{x=0}^{w} \mathrm{d}x} \tag{8}$$

$$= \frac{1}{w} \int_0^w \exp\left[+\xi x \frac{\sin(\alpha_i)\sin(\alpha_s)}{\cos(\alpha_i - \alpha_s)\cos(\alpha_i + \alpha_s)}\right] \mathrm{d}x \tag{9}$$

$$= \frac{1}{w} \left[\frac{\exp\left[+\xi x \frac{\sin(\alpha_i)\sin(\alpha_s)}{\cos(\alpha_i - \alpha_s)\cos(\alpha_i + \alpha_s)}\right]}{+\xi \frac{\sin(\alpha_i)\sin(\alpha_s)}{\cos(\alpha_i - \alpha_s)\cos(\alpha_i + \alpha_s)}}\right]_{x=0}^{w} \tag{10}$$

$$= \frac{\cos(\alpha_i - \alpha_s)\cos(\alpha_i + \alpha_s)}{\xi w \sin(\alpha_i)\sin(\alpha_s)} \left(\exp\left[+\xi w \frac{\sin(\alpha_i)\sin(\alpha_s)}{\cos(\alpha_i - \alpha_s)\cos(\alpha_i + \alpha_s)}\right] - 1\right) \tag{11}$$

In the limit of a well-focused beam impinging on the edge ($w \to 0$) the absorption asymmetry disappears. Similarly, for substrates of negligible absorption ($\xi \to 0$), this effect vanishes:

$$\lim_{\xi w \to 0} I_{+/-} \approx \frac{\cos(\alpha_i - \alpha_s)\cos(\alpha_i + \alpha_s)}{\xi w \sin(\alpha_i)\sin(\alpha_s)} \left(1 + \frac{1}{1!}\left[+\xi w \frac{\sin(\alpha_i)\sin(\alpha_s)}{\cos(\alpha_i - \alpha_s)\cos(\alpha_i + \alpha_s)}\right] + ... - 1\right) \tag{12}$$

$$\approx 1 \tag{13}$$

As an example of the magnitude of this effect, we consider realistic conditions for a GTSAXS experiment. For an incident angle of $\alpha_i = 0.20^\circ$ and a beam size of $100\,\mu m$, the projection is $w = (100\,\mu m)/\sin(\alpha_i) = 28.65\,\mathrm{mm}$. For a silicon substrate, the attenuation length at 13.5 keV is $\lambda_{\mathrm{att}} \approx 324\,\mu m$, or $\xi = 0.003086\,\mu m^{-1}$, and $\xi w = 88.4$.) Assuming scattering at $\alpha_s = 0.05^\circ$, we expect:

$$I_{+/-} = \frac{\cos(0.15^\circ)\cos(0.25^\circ)}{88.4 \sin(0.20^\circ)\sin(0.05^\circ)} \left(\exp\left[88.4 \frac{\sin(0.20^\circ)\sin(0.05^\circ)}{\cos(0.15^\circ)\cos(0.25^\circ)}\right] - 1\right) \tag{14}$$

$$\approx 1.00027 \tag{15}$$

This small correction can be neglected in most cases. A more extreme case is $\alpha_i = 1.50^\circ$ and $\alpha_s = 0.2^\circ$, which gives $I_{+/-} \approx 1.008$, or a 1% asymmetry.

Ewald Curvature Correction

The curvature of the Ewald sphere introduces an intensity correction to GTSAXS data, arising from the slightly asymmetric intersection of the tilted Ewald sphere with the reciprocal-space lattice-peaks. In general, the scattering above the direct beam will be more intense that the scattering below the direct beam, since the Ewald sphere is slightly closer to the (q_y, q_z) plane when $q_z > 0$.

$$q_x^2 + (q_y - k\cos\alpha_i)^2 + (q_z - k\sin\alpha_i)^2 - k^2 = 0 \tag{16}$$

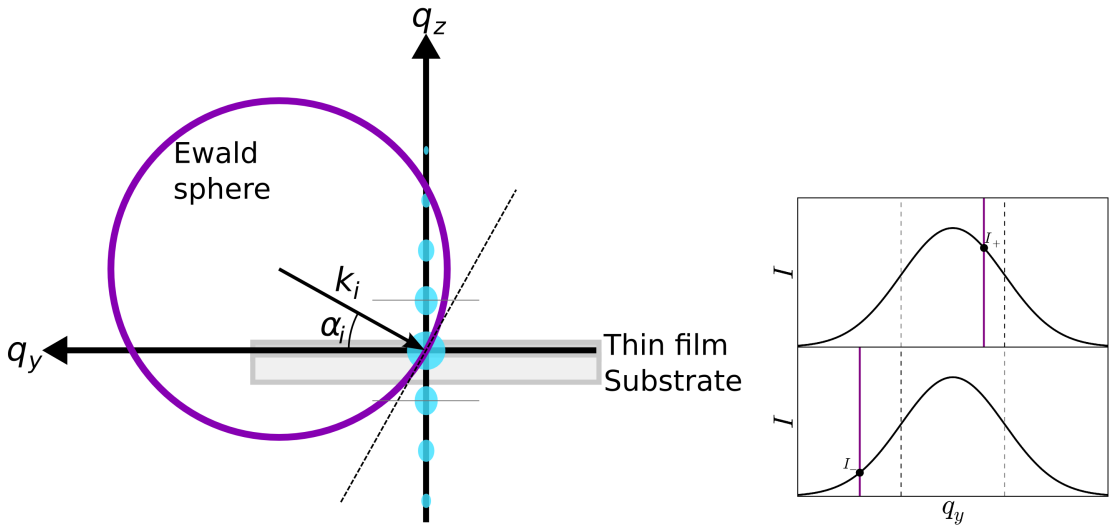

Figure 3: Ewald sphere in GTSAXS. The reflection angle tilts the Ewald sphere (purple) with respect to the sample's coordinate system. The sample's reciprocal-space scattering is represented by the blue lobes along the q_z axis (for illustrative purposes, it is assumed the scattering is concentrated into the (q_x, q_z) plane). The right graphs compare the experimentally-measured intensity for two mirror-image peaks. The intersection through the peak below the direct beam ($q_z < 0$) is further from the peak's center and thus sees a lower intensity. Note that when approximating the Ewald sphere as a plane (dashed line), the asymmetry would be ignored.

Consider now the effect of the curvature of the Ewald sphere on peaks localized to the (q_x, q_z) plane. For simplicity, we take the spread of these peaks from the plane as Gaussian:

$$I(q_x, q_y, q_z) = I(q_x, q_z) \frac{e^{-\frac{q_y^2}{2\sigma^2}}}{\sigma\sqrt{2\pi}} \tag{17}$$

Note that the function I is centrosymmetric in reciprocal-space (e.g. $I(q_x, q_y, +|q_z|) = I(q_x, q_y, -|q_z|)$). Consider now a pair of peaks, which on the detector plane are the same $|q_z|$ distance from the origin. To a first approximation, the intensity of the 'positive' peak (above the direct beam), $I_+ \equiv I(+q_z)$, is identical to the associated 'negative' peak (below the direct beam), $I_- \equiv I(-q_z)$. If the Ewald sphere is a perfectly flat plane, this equality ($I_+ = I_-$) holds; in the limit of small angles and/or small wavelength, this is a good approximation. However the curvature of the Ewald sphere does introduce a subtle correction, since for the 'positive' scattering peak the Ewald sphere intersects the scattering slightly *closer* to the (q_x, q_z) plane; whereas for the 'negative' peak, the intersection is slightly *further* from the (q_x, q_z) plane. More exactly:

$$I_+ = I(q_x, +|q_z|) \frac{e^{-\frac{q_{y,+}^2}{2\sigma^2}}}{\sigma\sqrt{2\pi}} \tag{18}$$

$$I_- = I(q_x, -|q_z|) \frac{e^{-\frac{q_{y,-}^2}{2\sigma^2}}}{\sigma\sqrt{2\pi}} \tag{19}$$

$$\tag{20}$$

Consider the form of $q_{y,+}$ and $q_{y,-}$ which results from the curvature of the Ewald sphere:

$$|q_y - k\cos\alpha_i| = +\sqrt{k^2 - q_x^2 - (q_z - k\sin\alpha_i)^2} \tag{21}$$

$$q_y - k\cos\alpha_i = -\sqrt{k^2 - q_x^2 - (q_z - k\sin\alpha_i)^2} \tag{22}$$

$$q_y^2 = \left(k\cos\alpha_i - \sqrt{k^2 - q_x^2 - (q_z - k\sin\alpha_i)^2}\right)^2 \tag{23}$$

Note that in eliminating the absolute value, we have selected the negative branch of the square-root since near the origin $(q_y - k\cos\alpha_i) < 0$. We now differentiate between the $+|q_z|$ and $-|q_z|$ peaks:

$$q_{y,+}^2 = \left(k\cos\alpha_i - \sqrt{k^2 - q_x^2 - (+|q_z| - k\sin\alpha_i)^2}\right)^2 \tag{24}$$

$$= k^2\cos^2\alpha_i - 2k\cos\alpha_i\sqrt{k^2 - q_x^2 - (+|q_z| - k\sin\alpha_i)^2} + k^2 - q_x^2 - (+|q_z| - k\sin\alpha_i)^2 \tag{25}$$

$$= k^2\cos^2\alpha_i - 2k\cos\alpha_i\sqrt{k^2 - q_x^2 - (|q_z| - k\sin\alpha_i)^2} + k^2 - q_x^2 - q_z^2 + 2k\sin\alpha_i|q_z| - k^2\sin^2\alpha_i \tag{26}$$

$$q_{y,-}^2 = k^2\cos^2\alpha_i - 2k\cos\alpha_i\sqrt{k^2 - q_x^2 - (-|q_z| - k\sin\alpha_i)^2} + k^2 - q_x^2 - (-|q_z| - k\sin\alpha_i)^2 \tag{27}$$

$$= k^2\cos^2\alpha_i - 2k\cos\alpha_i\sqrt{k^2 - q_x^2 - (|q_z| + k\sin\alpha_i)^2} + k^2 - q_x^2 - q_z^2 - 2k\sin\alpha_i|q_z| - k^2\sin^2\alpha_i \tag{28}$$

And note the difference of these quantities:

$$q_{y,-}^2 - q_{y,+}^2 = -2k\cos\alpha_i\sqrt{k^2 - q_x^2\left(q_z + k\sin\alpha_i\right)^2} - 2k\sin\alpha_i q_z \tag{29}$$

$$- \left(-2k\cos\alpha_i\sqrt{k^2 - q_x^2 - \left(q_z - k\sin\alpha_i\right)^2} + 2k\sin\alpha_i q_z\right) \tag{30}$$

$$= 2k\cos\alpha_i\left(\sqrt{k^2 - q_x^2 - \left(q_z - k\sin\alpha_i\right)^2} - \sqrt{k^2 - q_x^2\left(q_z + k\sin\alpha_i\right)^2}\right) - 4k\sin\alpha_i q_z \tag{31}$$

Inserting the above equations into the intensity ratio:

$$\frac{I_+}{I_-} = \frac{e^{-\frac{q_{y,+}^2}{2\sigma^2}}}{e^{-\frac{q_{y,-}^2}{2\sigma^2}}} \tag{32}$$

$$= \exp\left[+\frac{1}{2\sigma^2}\left(q_{y,-}^2 - q_{y,+}^2\right)\right] \tag{33}$$

$$= \exp\left[\frac{k\cos\alpha_i}{\sigma^2}\left(\sqrt{k^2 - q_x^2 - \left(q_z - k\sin\alpha_i\right)^2} - \sqrt{k^2 - q_x^2\left(q_z + k\sin\alpha_i\right)^2}\right) - \frac{2k\sin\alpha_i}{\sigma^2}q_z\right] \tag{34}$$

When the grazing angle is zero ($\alpha_i = 0$), symmetry is restored and $I_+/I_- = 1$. Similarly, in the limit of a broad distribution in q_y (which corresponds to low correlation in the y direction, either due to low beam coherence or poor sample ordering along that direction), the ratio tends to unity. In principle the intensity correction can be arbitrarily large, if the beam coherence and sample ordering are both extremely high. In practice, the instrumental resolution (which defines the width of the Ewald shell in reciprocal space) becomes a factor that limits σ to being a non-zero quantity.

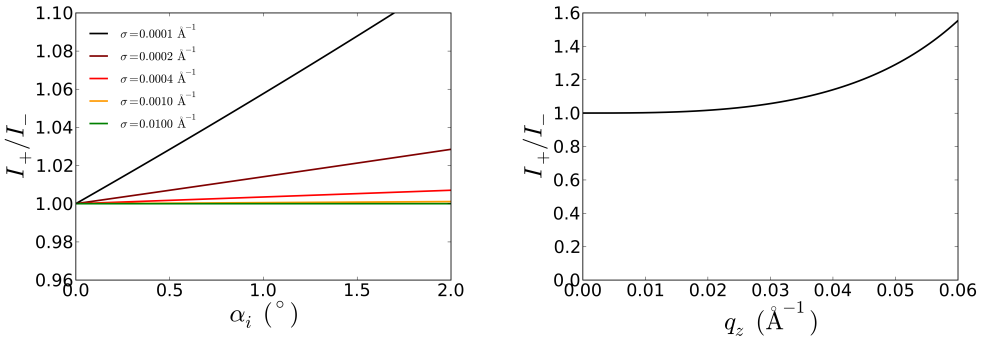

Figure 4: Estimates of the magnitude of the intensity correction due to Ewald curvature. Left: intensity ratio for $q_x = 0.0008$ Å^{-1} and $q_z = 0.006$ Å^{-1}. Right: Trend with q_z for $q_x = 0.006$ Å^{-1} and $\sigma = 0.0005$ Å^{-1}.

The figure estimates the magnitude of this effect for experimentally-realistic conditions. The resolution-limited σ for a typical experiment is of order 0.0005 Å^{-1}. In extreme cases it appears possible that an Ewald correction on the order of a few percent may be present. In cases where this correction is non-negligible, a non-linear correction to the measured intensities would be required.

In-plane Scattering Correction

Actual scattering peaks occur with both a vertical tilt with respect to the sample horizon (α_f) and an in-plane scattering angle (θ_f). We consider here whether the refraction correction is different for in-plane scattering peaks ($q_x \neq 0$), as compared to the correction for the direct beam ($q_x = 0$). The correction is found to be negligible.

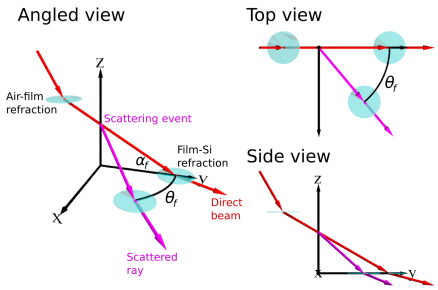

Figure 5: Geometry of scattering within a thin-film in GTSAXS.

In GTSAXS, the direct beam is refracted at both the air-film interface, and the film-substrate interface. Scattering events occurs within the film, and the scattered rays in general form an in-plane angle θ_f with respect to the direct beam. The scattered ray (like the direct beam) is refracted at the film-substrate interface. The in-plane rotation of the scattered ray means that the projected incident angle of the refracted beam is different from the direct beam. Thus the refraction effect seen at the detector plane changes with θ_f.

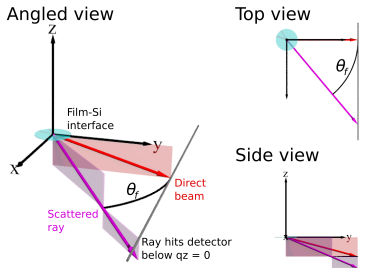

Figure 6: Geometry of scattering towards the detector plane in a GTSAXS experiment.

In the coordinate system of the detector, the scattered ray travels slightly further than the direct beam, and thus strikes the detector at a lower z-position. The magnitude of the effect is:

$$\delta z = D\left(\frac{1}{\cos\theta_f} - 1\right)\tan\alpha_f \tag{35}$$

Where D is the sample-detector distance. In a typical experiment, $q_x = 0.01$ Å^{-1} and $\theta_f \approx 0.08°$. So $\delta z < 1\,\mu m$, which is considerably smaller than typical detector pixel resolution. This correction to the refraction effect is thus entirely negligible.